THE JOURNAL OF BIOLOGICAL CHEMISTRY
Vol. 276, No. 16, Issue of April 20, pp. 12983–12990, 2001

Printed in U.S.A.

The Role of Water Molecules in the Association of Cytochrome P450cam with Putidaredoxin

AN OSMOTIC PRESSURE STUDY*

Received for publication, November 9, 2000, and in revised form, January 12, 2001
Published, JBC Papers in Press, January 12, 2001, DOI 10.1074/jbc.M010217200

Yoshiaki Furukawa and Isao Morishima‡

From the Department of Molecular Engineering, Graduate School of Engineering, Kyoto University, Kyoto 606-8501, Japan

We have investigated the osmotic pressure dependence of the association between ferric cytochrome P450cam and putidaredoxin (Pdx) to gain an insight into the role of water molecules in the P450cam-reduced Pdx complexation amenable to physiological electron transfer. The association constant was evaluated from the electron transfer rates from reduced Pdx to P450cam. The natural logarithm of the association constant K_a was linearly reduced by the osmotic pressure, and osmotic stress yields uptake of 25 waters upon association. In contrast, uptake of only 13 waters is observed from the osmotic pressure dependence of the association in the nonphysiological redox partners P450cam and oxidized Pdx. Although general protein-protein associations proceed through dehydration around the complex interface, the interfacial waters could mediate hydrogen-bonding interactions. Therefore, about 10 more interfacial waters imply an additional water-mediated hydrogen-bonding network in the P450cam·reduced Pdx complex, which does not exist in the complex with oxidized Pdx. It is also possible that the water-mediated hydrogen-bonding interactions support a high P450cam affinity for reduced (K_a = 0.83 μM^{-1}) relative to oxidized (K_a = 0.058 μM^{-1}) Pdx. This study points to a novel role of solvents in assisting redox state-dependent interaction between P450cam and Pdx.

The function of cytochrome P450cam (P450cam)[1] is to catalyze the stereoselective oxidation of camphor to 5-*exo*-hydroxycamphor (1). The full catalytic cycle of P450cam starts with NADH, which reduces the FAD-containing protein putidaredoxin reductase (PdR). PdR then transfers an electron to putidaredoxin (Pdx), and two distinct electron transfer (ET) steps are needed from Pdx to P450cam to enable catalysis. In the catalytic cycle, ferric P450cam tightly binds the reduced form of Pdx (Pdx^{red}), which is a catalytically competent complex, with a dissociation constant K_m of 1.6 μM (2), whereas the product after intracomplex ET (ferrous P450cam and oxidized Pdx (Pdx^{ox})), easily dissociates into the free forms (K_m = 88 μM) (2). Although the redox state-dependent affinity of P450cam with Pdx is necessary to efficiently inject an electron into the P450cam active site, the molecular mechanism of the recognition between P450cam and Pdx has not yet been proven in detail. In addition to being an electron shuttle to P450cam, Pdx is a conformational effector of P450cam (3). Low potential iron-sulfur protein such as spinach ferredoxin and bovine adrenodoxin can transfer a first electron to P450cam but not a second electron, resulting in a very slow turnover of the P450cam monooxygenase reaction. Therefore, many investigators have tried to characterize the association between P450cam and Pdx.

As yet, site-directed mutagenesis studies of amino acid residues on Pdx and P450cam have indicated that salt bridges are formed between Asp^{38} (Pdx) and Arg^{112} (P450cam) and Asp^{34} (Pdx) and Arg^{109} (P450cam) upon complexation (4–8). Computer modeling studies also support the importance of salt-bridge and hydrogen-bonding interactions upon P450cam-Pdx association (9, 10). Sligar and co-workers (2, 4, 11) have reported the mutational studies on the C-terminal residue Trp^{106} in Pdx and proposed that the presence of a C-terminal aromatic residue is required for the complex formation between P450cam and Pdx. Because a contribution to association energy from an aromatic residue is generally expected to come from desolvation of the residue in the complex, the elimination of water molecules from the P450cam·Pdx complex interface is plausible. Such a partial desolvation of the aromatic residue in the binding cleft could accompany the decrease in the dielectric constant for the binding region, which results in the increase of the magnitude of any existing electrostatic interactions. Therefore, not only the simple salt-bridge and hydrogen-bond formation, but also the water molecules at the P450cam·Pdx complex interface should be important for molecular recognition between P450cam and Pdx. However, little attention has so far been paid to the role of water molecules in the P450cam-Pdx association reaction.

Because bound water molecules appear to form an integral part of the structure of proteins and their complexes with partner proteins, solvent has been shown to play a significant role in biologically important protein association systems. For example, upon ferredoxin-ferredoxin:$NADP^+$ reductase association, the large positive entropy changes (+157 J mol^{-1} K^{-1}) with small, unfavorable enthalpy changes were observed by Jelesarov and Bosshard (12). Most protein-protein associations in the ET reactions show large positive entropy changes of binding by excluding water molecules from the complex interface (13–15). In contrast, our group (16) has reported that the energetics of the P450cam-Pdx association is characterized by a favorable enthalpy change (ΔH = −53.8 kJ mol^{-1}) and a neg-

* This work was supported by a Grant-in-aid for Scientific Research on Priority Areas from the Ministry of Education, Science, Sports, and Culture of Japan 08249102 (to I. M.). The costs of publication of this article were defrayed in part by the payment of page charges. This article must therefore be hereby marked "*advertisement*" in accordance with 18 U.S.C. Section 1734 solely to indicate this fact.

‡ To whom correspondence should be addressed: Dept. of Molecular Engineering, Graduate School of Engineering, Kyoto University, Kyoto 606-8501, Japan. Tel.: 81-75-753-5921; Fax: 81-75-751-7611; E-mail: morisima@mds.moleng.kyoto-u.ac.jp.

[1] The abbreviations used are: P450cam, cytochrome P450 camphor; PdR, putidaredoxin reductase; Pdx, putidaredoxin; ET, electron transfer; MV, methyl viologen.

ative entropy change ($\Delta S = -93.2$ J mol^{-1} K^{-1}) of binding. With respect to the negative entropy change in the P450cam-Pdx association, it is plausible that the water molecules are trapped rather than excluded at the complex interface between P450cam and Pdx.

To gain insights into the molecular recognition between P450cam and Pdx, we examined the contribution of interfacial water molecules to P450cam-Pdx association by using the osmotic stress strategy (17). Decreasing the water activity of the bulk solution by using osmolytes can shift the equilibrium between the unbound proteins and its complex because protein-protein interfaces behave as though they are separated from the bulk solution by a semipermeable membrane, the protein itself. That is, high osmotic pressure promotes dehydration of the molecular surface and should promote binding if water is released from the complex interface. Similarly, if interfacial water stabilizes binding, a decrease in water activity will decrease the binding affinity.

Di Primo *et al.* (18) have reported the osmotic pressure dependence on the NADH consumption rate in the P450cam catalytic cycle and observed the decreased turnover under high osmotic pressure. However, a number of steps in the P450cam catalytic cycle inhibit the detailed characterization of the relationship between P450cam-Pdx association and the water molecules. In this study, we measured the rate of the interprotein ET from Pdx^{red} to ferric P450cam, which is a more specific measurement of the association constant of the physiological complex, ferric P450cam·Pdx^{red}. Furthermore, by spectrophotometric examination of the osmotic pressure dependence of the nonphysiological association between ferric P450cam and Pdx^{ox}, the role of water molecules in the recognition of P450cam to Pdx is discussed.

EXPERIMENTAL PROCEDURES

Preparation of Cytochrome P450cam and Putidaredoxin—P450cam was expressed in *Escherichia coli* strain JM83 having the pUC18 vector and purified with the procedures previously described (19). Purified preparations with an RZ value (A_{391}/A_{280}) greater than 1.4 were employed in this study. Pdx was expressed in *E. coli* strain RR1 as described elsewhere (8).

Measurement of the Electron Transfer Rate Constants—Laser flash photolysis experiments utilized the third harmonic (355 nm) of a Q-switched Nd:YAG laser, which provides photolysis pulses with a half-peak duration of 10 ns. The monitoring beam was generated by a xenon lamp (150 watt) and focused on the sample cell at the right angle of the excitation source through a notch filter. The transmitted light was detected by a photomultiplier that is attached to a monochrometer, UNISOKU USP-501. A two-channel oscilloscope (TDS320) was used to digitize and accumulate the signals that were transferred to a NEC PC-98 computer for the further analysis. Temperature was controlled by using a circulating water bath.

Scheme 1 shows the photochemical reaction in which the acridine triplet and the methyl viologen (MV) initiate protein-protein ET (20). Briefly, a laser flash at 355 nm excites acridine to its triplet state, which in turn oxidizes EDTA, resulting in formation of acridine semiquinone in less than 1 μs. Following that, the photoreduced acridine reduces methyl viologen (MV), to form the MV cation radical. Then, the MV cation radical reduces Pdx^{ox} some hundred times faster than ferric P450cam in the mixture of P450cam and Pdx (See "Results"). Finally, the ET reaction from Pdx^{red} to ferric P450cam can be monitored as the formation of ferrous carbonyl P450cam (P450cam–CO) under CO atmosphere. Sample solutions for the laser experiments were degassed and purged with CO under vacuum. Because the reaction product, P450cam–CO, is accumulated by laser flash, we adopted the data of the kinetic trace from one laser flash for further analysis. The experiments were repeated for five times to estimate the experimental error. The kinetic measurements were performed at 293 K in a CO-saturated solution containing 10 μM Pdx^{ox}, 5–25 μM ferric P450cam, 15 μM acridine, 500 μM MV, 25 mM EDTA, 50 mM potassium phosphate, 1 mM *d*-camphor, pH 6.7.

Preparation of Sample Solution Buffers—Preparation of the solution buffers containing cosolvents for laser experiments were accomplished as follows. 50 mM potassium phosphate buffers containing 12, 16% (w/w) glycerol, 8, 16% (w/w) ethylene glycol, or 15, 30% (w/w) glucose, were prepared. Acridine and *d*-camphor were completely dissolved in the aqueous buffer. The concentration of acridine in the solution buffers was checked spectrophotometrically ($\epsilon_{353} = 17$ mM^{-1} cm^{-1}). Following that, MV and EDTA were added, and the pH of the solution was checked. In the case of the buffers containing glucose, the pH of the solution was decreased to about 6.0 with the addition of EDTA. Because the pH of the other cosolvent-containing solutions was 6.7, we adjusted the pH of glucose-containing buffers to 6.7 with concentrated KOH solution.

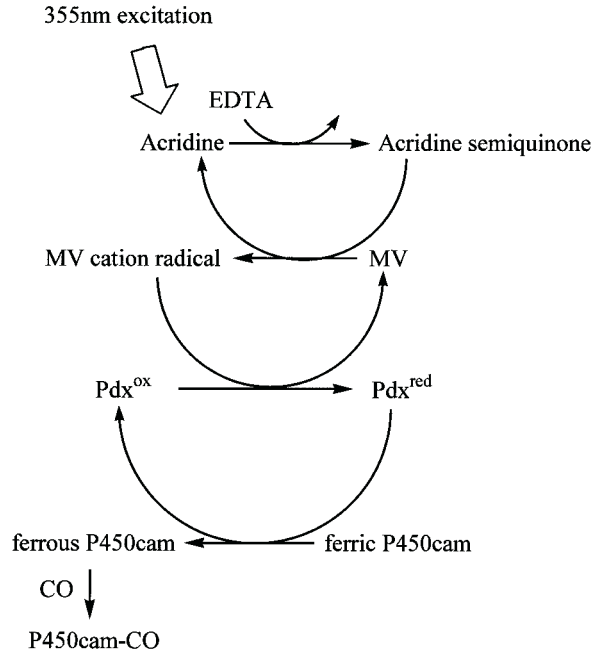

SCHEME 1.

Analysis of the Electron Transfer Rate Constants—To obtain the association and the ET rate constants between ferric P450cam and Pdx^{red}, we followed the analysis method of Davies and Sligar (2). The three-state model appropriate to the Pdx-P450cam enzyme system is shown in Reaction 1.

$$A + B \underset{k_{-1}}{\overset{k_1}{\rightleftharpoons}} C \underset{k_{-ET}}{\overset{k_{ET}}{\rightleftharpoons}} D$$

REACTION 1

In this reaction scheme, Pdx^{red} and ferric P450cam are the associating species A and B. Species C corresponds to the reactant complex, and D represents the bound and unbound product proteins, Pdx^{ox} and P450cam–CO. As previous studies have shown (21), the bimolecular association step is sufficiently faster than the ET step in the complex in the reaction between P450cam and Pdx. In such a case, the observed rate constants of the formation of P450cam–CO can be expressed by the sum of the concentrations of each unbound reactants at equilibrium as in the following equation,

$$k_{obs} = \frac{k_{ET}([\overline{Pdx^{red}}] + [\overline{\text{ferric P450cam}}])}{\frac{1}{K_a^{red}} + [\overline{Pdx^{red}}] + [\overline{\text{ferric P450cam}}]} + k_{-ET} \qquad \text{(Eq. 1)}$$

where $K_a^{red} = (k_1/k_{-1})$ is the association constant between ferric P450cam and Pdx^{red}. It has been reported that the value of k_{-ET} is essentially zero in the experimental system used in this study because the presence of CO effectively prevents the reversal of this reaction (21). The summed equilibrium concentrations of Pdx^{red} and ferric P450cam were estimated from the amplitude of the reaction progressive curves. Briefly, the concentrations of Pdx^{red} generated by a laser pulse, $[Pdx^{red}]_o$, was estimated in the absence of P450cam from the absorbance change at 420 nm (Fig. 1*A*), a wavelength at which there is a significant bleach in the (Pdx^{red} minus Pdx^{ox}) redox difference spectrum ($\Delta\epsilon_{420} = -5.83$ mM^{-1} cm^{-1}). The P450cam–CO concentration, [P450cam–CO], generated by the ET reaction with Pdx^{red} was also determined by the

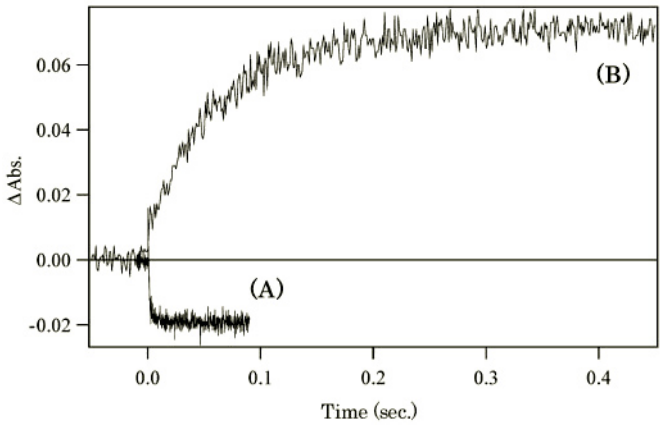

FIG. 1. **Transient absorbance changes at 420 nm obtained after a 355-nm laser excitation of Pdx^{ox} (*A*) and ferric P450cam (*B*) at 293 K.** The sample solution contains 10 μM protein in 50 mM KP_i, 1 mM *d*-camphor, 15 μM acridine, 500 μM MV, 25 mM EDTA, pH 6.7

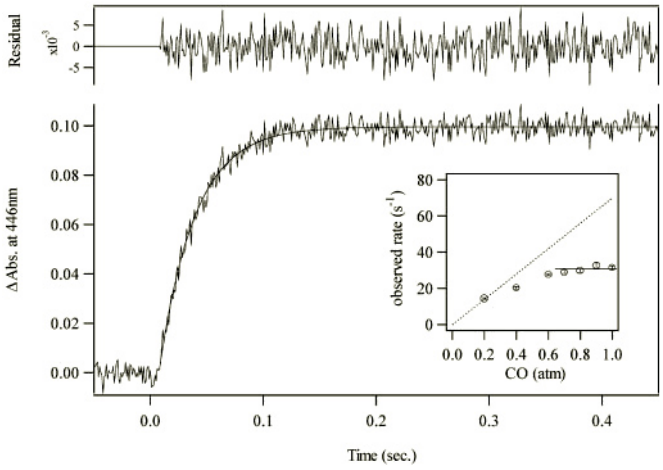

FIG. 2. **Transient absorbance change at 446 nm obtained after a 355-nm laser excitation under CO-saturated atmosphere of 15 μM ferric P450cam in the presence of 10 μM Pdx^{ox}.** The residuals of the single-exponential fitting are shown above the signals. The experiments were performed at 293 K, and the proteins were dissolved in 50 mM KP_i, 1 mM *d*-camphor, 15 μM acridine, 500 μM MV, 25 mM EDTA, pH 6.7. *Inset*, CO partial pressure dependence of the observed rate constants. The *dashed line* shows the CO rebinding rate constants of P450cam.

absorbance change at 446 nm (Fig. 2), where P450cam–CO dominantly absorbs ($\Delta\epsilon_{446}$ = 106.6 mM^{-1} cm^{-1}). Because the ET reaction between Pdx^{red} and ferric P450cam occurs through the 1:1 complex (9, 21, 22), the concentration of Pdx^{red} or ferric P450cam at equilibrium can be expressed as follows,

$$[\overline{\text{Pdx}^{red}}] = [\text{Pdx}^{red}]_o - [\text{P450cam–CO}] \quad \text{(Eq. 2)}$$

$$[\overline{\text{ferric P450cam}}] = [\text{ferric P450cam}]_o - [\text{P450cam–CO}] \quad \text{(Eq. 3)}$$

where [ferric P450cam]$_o$ is the concentration of ferric P450cam in the sample before a laser pulse.

Measurement of the Dissociation Constant of Ferric P450cam with Pdx^{ox}—The methods of Hintz *et al.* (22) were used to measure the dissociation constant of ferric P450cam with Pdx^{ox}. The sample cuvette contained 1500 μl of 50 mM potassium phosphate, pH 6.7, containing 1 mM *d*-camphor with cosolvents and 2 μM ferric P450cam. The reference cuvette also contained 1500 μl of the same solution except for P450cam. About 5 mM Pdx^{ox} was added stepwise to both cuvettes up to 25 μl. The measurements were carried out at room temperature. The binding of Pdx^{ox} to ferric P450cam induces a spectral change that is characterized by a decrease and increase in absorption around 390 and 420 nm, respectively. This spectral change indicates a Pd-induced spin-state shift of the ferric P450cam from high-spin to low-spin. The free Pdx concentration, $[\text{Pdx}]_{free}$, was calculated by Equation 4 (23).

$$[\text{Pdx}]_{free} = [\text{Pdx}]_{total} - \left(\frac{\Delta A_{391}}{\Delta A_{391\,max}}\right) \cdot [\text{P450cam}] \quad \text{(Eq. 4)}$$

The reciprocal of the absorbance change at 391 nm was then plotted against the reciprocal of free Pdx^{ox} concentrations, and the spectroscopic dissociation constant, K_s, was calculated.

Analysis of the Association Step in the Presence of Osmolytes—To examine the effects of the osmotic pressure on the association constants K_a between P450cam and Pdx, we used three kinds of osmolytes as performed by Di Primo *et al.* (18); glycerol, ethylene glycol, and glucose. The osmotic pressure, P_{osm}, for the solvent at different osmolyte contents was estimated using Equation 5,

$$P_{osm} = \frac{RT}{V_{H_2O}} \times \ln X_{H_2O} \quad \text{(Eq. 5)}$$

where X_{H_2O} and V_{H_2O} are the mole fraction and the molar volume of water, respectively. X_{H_2O} was calculated using tabulated values of the water content for each osmolyte/water mixtures (24). For V_{H_2O}, a value of 18 ml/mol was used. To quantitatively characterize the osmotic pressure dependence of the association process between P450cam and Pdx, we estimated the volume change associated with the osmotically available water in the two states of the equilibrium, ΔV_W, which is defined by Equation 6 (25).

$$\left(\frac{\partial \ln K_a}{\partial P_{osm}}\right)_T = -\frac{\Delta V_W}{RT} \quad \text{(Eq. 6)}$$

RESULTS

Upon flash photolysis of acridine/EDTA/MV solution, we found an absorbance increase at 700 nm in a μs time scale, which is the wavelength maximum for the MV cation radical (data not shown). In the absence of an electron-accepting species, P450cam or Pdx, the MV cation radical was stable for more than 500 ms. The MV cation radical can reduce Pdx^{ox} about 100× faster than ferric P450cam (20). For example, 1.5 μM MV cation radical can reduce Pdx^{ox} at 1250 s^{-1} in the presence of 10 μM Pdx^{ox}, whereas the reduction of 10 μM P450cam occurs with a much slower rate constant, 15 s^{-1} (Fig. 1). Concomitant with the reduction of Pdx^{ox} or ferric P450cam, the MV cation radical was oxidized to its original state, MV, with a similar rate constant to the reduction rate of Pdx^{ox} or ferric P450cam, showing that the MV cation radical donates an electron to Pdx^{ox} or ferric P450cam (data not shown). The faster reduction of Pdx^{ox} over P450cam by the MV cation radical was confirmed in the all cosolvent concentrations examined in this study.

Even in the solution containing both Pdx^{ox} and P450cam, an electron was favorably transferred from the MV cation radical to Pdx^{ox}. In the presence of 10 μM Pdx^{ox} in the sample, MV cation radical decays with the same rate constant, regardless of the absence or the presence of P450cam. This decay rate is accelerated about 2-fold, when the solution contains 20 μM Pdx^{ox}. These data imply that the MV cation radical first reacts with Pdx^{ox}, and the favorable reduction of P450cam by MV cation radical is less possible under the experimental conditions in this study.

In addition, we observed the redox process of Pdx to ensure the favorable reduction of Pdx by MV cation radical in the presence of P450cam. Lacking Pdx in the sample solution, only the increase of the absorbance at 467.4 nm, which is the isosbestic point between ferrous P450cam and P450cam–CO,[2] was

[2] A small amount of P450cam–CO sometimes exists before the laser experiment partially because of the room light. Such preformed P450cam–CO is converted to the ferrous form by the laser irradiation. To eliminate the small contribution by the absorbance change from P450cam–CO to ferrous P450cam, the measurements for the Pdx redox process were done at the isosbestic point, 467.4 nm, between ferrous P450cam and P450cam–CO.

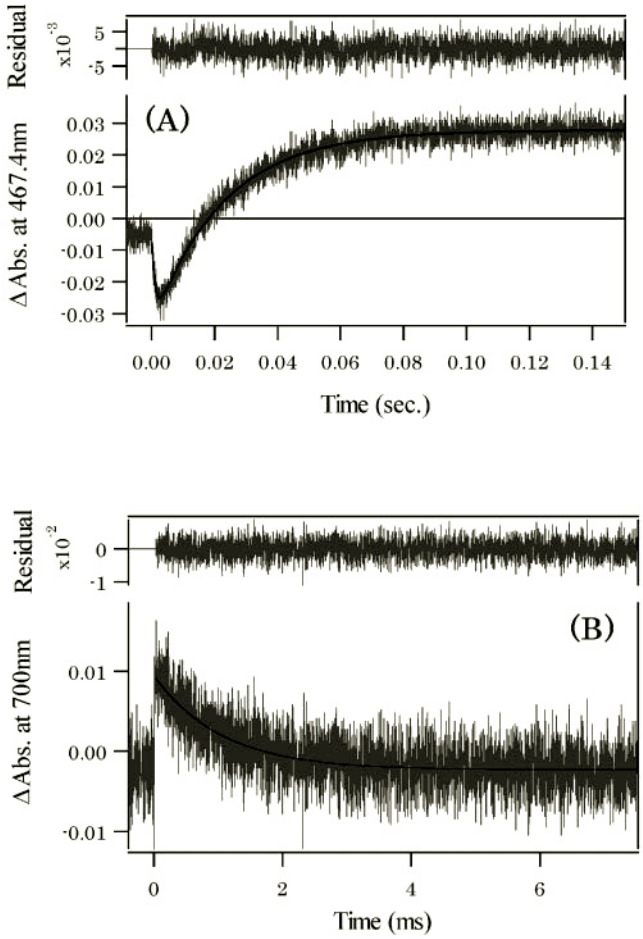

FIG. 3. **Transient absorbance change at 467.4 nm (*A*) and 700 nm (*B*) obtained after a 355-nm laser pulse.** The residuals of the double-exponential (*A*) or the single-exponential (*B*) fitting are shown at the *top* of the figure. Conditions; 10 μM Pdx^{ox}, 20 μM P450cam in 50 mM KP_i, 1 mM *d*-camphor, 15 μM acridine, 500 μM MV, 25 mM EDTA, pH 6.7.

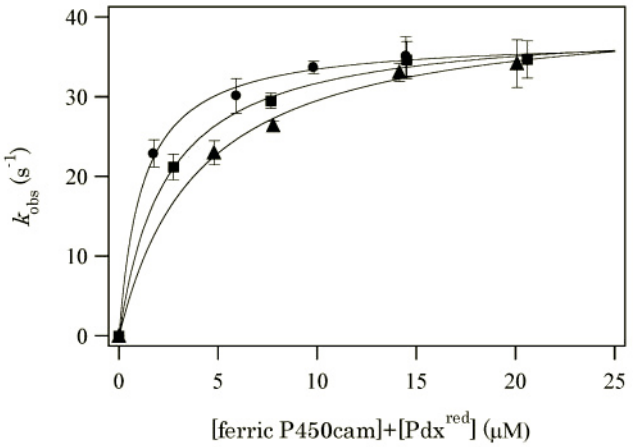

FIG. 4. **The dependence of the observed rate constant on the summed equilibrium concentration of Pdx^{red} and ferric P450cam in the free states.** *Circle*, the absence of the cosolvent; *square*, 12% (w/w) glycerol; *triangle,* 16% (w/w) glycerol. The *solid curve* is the least squares fit to the data using Eq. 1 (See "Experimental Procedures").

observed by a laser shot, indicating the formation of P450cam–CO by laser-generated MV cation radical. When the reaction mixture further contains 10 μM Pdx, the absorbance changes at 467.4 nm initially decrease by laser shot and show the subsequent gradual increase (Fig. 3*A*). Because there is significant bleach at 467.4 nm in the static difference spectrum of reduced minus oxidized Pdx, the initial decrease by laser shot indicates the reduction of Pdx. The rate constants of the reduction of Pdx are essentially the same as those of the MV cation radical decay estimated from the absorbance changes at 700 nm (Fig. 3*B*), which indicates that MV cation radical favorably donates an electron to Pdx^{ox} even in the presence of the excess P450cam (10 μM Pdx and 20 μM P450cam). The gradual increase of the 467.4 nm absorption means both of the re-oxidation of Pdx^{red} and the formation of P450cam–CO. The single exponential function was adequate to fit this absorption increase, which implies that Pdx^{red} donates an electron to P450cam and the ET from MV cation radical to P450cam have little contribution to the observed kinetics.

From these results, the MV cation radical primarily reduces Pdx^{ox} in the mixture of P450cam and Pdx, as suggested previously (20). This aspect of reduction reactions by MV cation radical will reflect the difference in the electrostatic potentials on the surface near the redox center of each protein (26). The best position on the surface of P450cam for ET reactions is a positive charged domain, whereas Pdx carries a negative charge near the redox center [2Fe–2S] cluster. Because the MV cation radical bears the positive charge, the favorable electrostatic interaction with negatively charged Pdx makes the reduction faster because of a closer spatial distance between redox centers.

The kinetic trace shown in Fig. 2 illustrates the formation of P450cam–CO under CO-saturated conditions in the presence of 15 μM ferric P450cam and 10 μM Pdx^{ox}. Many studies have clarified that the equilibration of Pdx^{red}·ferric P450cam complex is fast relative to the ET process in the complex (Reaction 1, Refs. 21, 22). Also, the CO-binding step in ferrous P450cam will not be rate-limiting under the conditions of saturated CO used in this study (21). As shown in the *inset* of Fig. 2, the observed rate constants are independent of CO partial pressure in the range between 0.6 and 1.0 atm. Whereas the CO-binding to P450cam becomes a limiting step in the low CO partial pressure, this result clearly indicates that the experimental condition of the saturated CO atmosphere permits the observation of the ET process from Pdx^{red} to P450cam.

We also confirmed little effect by the small molecules (MV, acridine, glycerol, ethylene glycol, and glucose) on the CO binding process in P450cam under the saturated CO atmosphere. A laser pulse dissociates CO from P450cam–CO, which is prepared by addition of dithionite, to form ferrous P450cam. Following that, ferrous P450cam rebinds CO with a rate constant of 70 s^{-1} in the 50 mM potassium phosphate/1 mM *d*-camphor, pH 6.7. Even when the cosolvents are present, the CO rebinding rate constants remain virtually unchanged; 70 s^{-1} in 500 μM MV/15 μM acridine, 16% ethylene glycol, or 30% glucose, 60 s^{-1} in 16% glycerol. The CO-binding process is, therefore, not affected by the cosolvent concentrations used in this study. The P450cam–CO formation rate shows saturation behavior against the concentration of P450cam (Fig. 4), which is more evidence that the CO-binding step is not rate-limiting. Therefore, the formation of P450cam–CO in this experiment follows the events of the ET reaction step in the Pdx^{red}·ferric P450cam complex.[3]

[3] We also observed the kinetics of ferric P450cam by monitoring the absorbance change at 650 nm. The ferric form of P450cam has a charge-transfer band at 650 nm, whereas the ferrous and CO-form of P450cam do not. In all conditions used in this study, a laser pulse decreases the absorption at 650 nm with the same rate constant as that obtained from the absorbance change at 446 nm. As discussed by Hintz et al. (21), this is consistent with the expectation that the CO-binding process is not the rate-determining step under our experimental conditions.

TABLE I
Association constants, K_a^{red} and K_a^{ox} and electron transfer rate constants, k_{ET}, between ferric P450cam and reduced Pdx under various cosolvent concentrations

	P_{osm}	$K_a^{red} \times 10^2$	k_{ET}	$K_a^{ox} (= 1/K_s) \times 10^2$
	MPa	μM^{-1}	s^{-1}	μM^{-1}
0% cosolvent	0	83 ± 14	37 ± 1.0	5.8 ± 0.52
12%(w/w) glycerol	3.7	42 ± 7.0	39 ± 1.0	4.7 ± 0.50
16%(w/w) glycerol	5.3	25 ± 6.0	41 ± 2.5	3.5 ± 0.54
15%(w/w) glucose	2.4	45 ± 16	38 ± 2.0	4.4 ± 0.39
30%(w/w) glucose	6.2	24 ± 1.0	38 ± 0.1	3.0 ± 0.28
8%(w/w) ethylene glycol	3.4	29 ± 4.0	41 ± 4.1	4.3 ± 0.43
16%(w/w) ethylene glycol	7.6	19 ± 3.0	45 ± 2.0	2.9 ± 0.41

Association of Ferric P450cam with Pdx^{red}—The kinetic traces of P450cam–CO formation can be well fitted by a single-exponential function (Fig. 2), which is also the case for the traces in all cosolvent concentrations. By plotting the observed rate constants as a function of the sum of Pdx^{red} and ferric P450cam concentrations at equilibrium (Eq. 1, Fig. 4), we obtained an association constant, K_a^{red}, and an ET rate constant, k_{ET}, in the ferric P450cam·Pd^{red} complex under various cosolvent concentrations as summarized in Table I. The obtained values of k_{ET} and K_a^{red} without cosolvent molecules are consistent with those reported previously (2, 6). The addition of cosolvents decreases the association constant, K_a^{red}, and has little effect on k_{ET}. K_a^{red} changed from 0.83 μM^{-1} (in the absence of cosolvents) to 0.19 μM^{-1} (16% ethylene glycol), whereas the changes in k_{ET} are small and in the range between 37 and 45 s^{-1}. The effects of cosolvents are, therefore, mainly on the association process but not on the ET process. Fig. 5*A* shows the plot of association constant against osmotic pressure, and ln K_a^{red} scales down as a linear function of osmotic pressure (R^2 = 0.903), which means that the increase in osmotic pressure destabilizes the complex between Pdx^{red} and ferric P450cam. However, the poor correlations with the changes in K_a^{red} were found against the other solvent colligative properties, such as the viscosity (R^2 = 0.235), the dielectric constant (R^2 = 0.507), or the water molarity (R^2 = 0.662). In addition, the variety of cosolvents (glycerol, ethylene glycol, glucose) tested rules out a specific interaction between the cosolvent molecules and the P450cam·Pdx complex. Osmotic stress (Eq. 6) yields a value for ΔV_W of 457 ± 99 cm^3/mol. Assuming a partial molar volume of water equal to 18 cm^3/mol, the obtained value, 457 ± 99 cm^3/mol, would correspond to 25 ± 6 molecules of osmotically active water involved in the association process.

Association of Ferric P450cam with Pdx^{ox}—Fig. 6 shows the Pdx^{ox}-induced difference spectra for ferric P450cam without cosolvents. Complexation with Pdx^{ox} decreases the absorbance around 390 nm and increases the absorbance around 420 nm. This Pdx effect has been observed previously (27) and serves as an indicator of complex formation between ferric P450cam and Pdx^{ox}. As depicted in the *inset* to Fig. 6, in all cosolvents used, the reciprocal of the absorbance decrease at 391 nm is linearly correlated with the reciprocal of the concentration of free Pdx^{ox}. In the absence of any cosolvents, the spectroscopic dissociation constant, K_s, was 17.2 ± 1.4 μM, which is consistent with the previously reported values (28, 29). By adding the cosolvents, glycerol, ethylene glycol, and glucose, K_s was increased, as summarized in Table I. As seen in the case of ferric P450cam-Pdx^{red} association, linear correlation was also observed between the natural logarithm of the association constant in ferric P450cam/Pdx^{ox} ($K_a^{ox} = 1/K_s$) and the osmotic pressure (R^2 = 0.923). The ln K_a^{ox} is poorly correlated with the other solution properties; R^2 = 0.464 (relative viscosity), 0.746 (dielectric constant), 0.846 (water molarity). By using Eq. 6, we obtained 230 ± 30 cm^3/mol as ΔV_W, and the number of trapped osmotically labile water molecules can be estimated as about 13 ± 2 upon association of ferric P450cam with Pdx^{ox}.

DISCUSSION

As shown in Table I, addition of the cosolvents to the solution leads to an increase in the osmotic pressure, which disfavors the interactions between ferric P450cam and Pdx irrespective of the redox state. Previous studies have revealed that the osmotic pressure perturbs the spin equilibrium of ferric P450cam and favors the high-spin form by excluding the water molecules in the P450cam active site (30). The dehydrating effect of increasing osmotic pressure on ferric P450cam (camphor-bound) was also observed in this study (data not shown). Because the high and low spin forms of ferric P450cam represent two conformational states of the protein (31), it is possible that the P450cam conformational changes induced by osmotic pressure reduce the association between ferric P450cam and $Pdx^{ox/red}$. In such a case, the osmotic pressure dependence of the association of ferric P450cam would be the same between ferric P450cam·Pdx^{ox} and ·Pdx^{red} complexes. The different volume changes, however, are observed for ferric P450cam·Pdx^{red} (ΔV_W = 457 cm^3/mol) and ferric P450cam·Pdx^{ox} (ΔV_W = 230 cm^3/mol), which implies that the osmolyte-induced conformational changes are not the major origins of the reduced association.

Moreover, the substantial conformational changes might be expected to influence the ET rate constant in the ferric P450cam·Pdx^{red} complex, because the ET rate constant is very sensitive to the distance and the orientation between the two redox proteins. According to the Marcus theory (32), which is often applied to the analysis of the protein ET reactions, only the 0.5 Å elongation of the distance is predicted to result in the 2-fold reduction in the ET rate constant. Against such an expectation, the observed ET rate constant is almost unchanged up to 10 MPa (Table I), showing that the osmotic pressure makes a smaller perturbation on the structure of the P450cam·Pdx complex. As to Pdx, its UV/vis spectrum is not affected by osmotic pressure, and the redox potential is also unchanged (data not shown). It is, therefore, unlikely that the reduced association between ferric P450cam and $Pdx^{ox/red}$ is caused by the protein conformational changes induced by osmotic pressure.

Application of osmotic pressure relies upon the existence of a water-permeable barrier (the complex interface in this study) separating a population of water molecules from a nonpermeating solute, osmolyte (17). Correlation of a process with osmotic pressure implies a change in the size of this population. Previous studies have shown that most protein-protein association processes in the ET reactions are usually accompanied by the release of water molecules from the interface of the complex through the hydrophobic interactions (12, 33–36). The increase of osmotic pressure leads to the increase of its association constants because of the desolvation at the complex interface, as seen in the cytochrome b_5-cytochrome *c* association reaction (ΔV_W = −47 cm^3/mol) (34). Therefore, the simplest interpretation of the reduced association by osmotic pressure is that a population of bound waters, sequestered from bulk solvent, is present at the P450cam·Pdx complex interface but is not present in the free states of P450cam or Pdx.

Comparison with Previous Thermodynamic Studies—The uptake of water molecules would be supported by our recent thermodynamic studies on the binding between ferric P450cam and Pdx^{ox} (16). Our group has reported that the binding energetics of the ferric P450cam·Pdx^{ox} complex is characterized by the negative entropy change (ΔS = −93.2 J mol^{-1} K^{-1}). It has

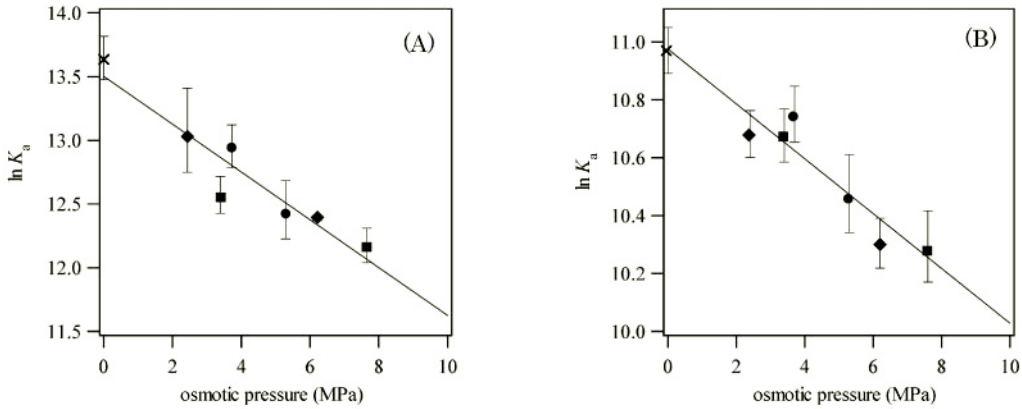

FIG. 5. **Dependence of the association constants on the osmotic pressure for ferric P450cam binding to Pdx^{red} (*A*) and Pdx^{ox} (*B*) for the three osmolytes: glycerol (*circle*), ethylene glycol (*square*), glucose (*diamond*), and in the absence of cosolvent (*cross*).** The *solid line* represents the best fits by linear regression using Eq. 6.

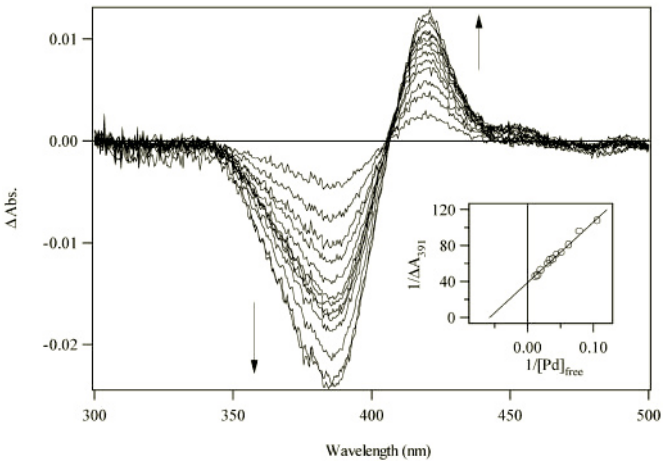

FIG. 6. **Difference spectra of 2 μM ferric P450cam with addition of Pdx^{ox} at room temperature in 50 mM KP_i, 1 mM *d*-camphor, pH 6.7.** The spin-state shift of ferric P450cam from high- to low-spin induced by the binding of Pdx^{ox} is clearly observed. The final concentration of Pdx^{ox} is 86 μM. *Inset,* double-reciprocal plot of titration of ferric P450cam with Pdx^{ox} in the absence of cosolvents. Details are described under "Experimental Procedures."

been suggested that the decreased entropy is partially caused by the ordering of water molecules in and around the protein-protein interface. Xavier *et al.* (37) have estimated the number of water molecules trapped in the association between bobwhite quail lysozyme and the monoclonal antibody HyHEL-5 by using the experimental data of the entropy changes of binding. Following their method (37, 38), the entropy change of binding can be expressed as the sum of the three types of entropy changes; the hydrophobic effect, ΔS_{hydr}, the decrease in the rotational and translational degrees of freedom, ΔS_{trans}, and the other contributions, ΔS_{other} as shown in Equation 7.

$$\Delta S = \Delta S_{hydr} + \Delta S_{trans} + \Delta S_{other} \quad \text{(Eq. 7)}$$

As discussed by Xavier *et al.* (37), the entrapment of water molecules at the complex interface would be reflected by the term, ΔS_{other}. ΔS_{hydr} can be estimated by using the following relationship (39),

$$\Delta S_{hydr} = 1.35 \Delta C_p \ln\left(\frac{T}{386}\right) \quad \text{(Eq. 8)}$$

where ΔC_p is the measured heat capacity change. Studies in statistical mechanics and the experiments on different protein-protein associations show that ΔS_{trans} is approximately -209 J mol^{-1} K^{-1} (40, 41). Because ΔS and ΔC_p in the association of ferric P450cam with Pdx^{ox} were determined as -93.2, -1290 J mol^{-1} K^{-1}, respectively (16), ΔS_{other} is estimated as about -364 J mol^{-1} K^{-1}. Dunitz (42) has used the entropy of water in ice and hydrates of various salts to arrive at an upper limit for the entropy of water tightly bound to the surface of a protein as 29.3 J mol^{-1} K^{-1}. Using this value and assuming that all of ΔS_{other} is attributed to water uptake, an estimate of 12 trapped water molecules is obtained. This number of the water molecules is in good agreement with that obtained by the osmotic stress experiments in this paper (13 $\pm$ 2 water molecules). Both the osmotic pressure experiments and the calorimetric studies, therefore, indicate the important contribution of water molecules to the P450cam-Pdx interaction.

Role of the Interfacial Water Molecules in the P450cam·Pdx Recognition—So far, the uptake of water molecules has been studied in the following systems; the binding of cytochrome *c* by cytochrome *c* oxidase (ΔV_W = 224 cm^3/mol) (34), the binding of lysozyme with its antibody (ΔV_W = 216 cm^3/mol) (37), and several protein-DNA complexes (43). For example, Bhat *et al.* (44) reported the 1.8 Å-resolution crystal structure of the complex of hen egg white lysozyme (HEL) with its antibody Fv D1.3, and found that the trapped water molecules at the interface bridge two proteins by making hydrogen bonds with protein residues. They also proposed that these water-mediated hydrogen bonds contribute to the stabilization and the high specificity of the antigen-antibody complex.

In the P450cam·Pdx complex, the formation of five direct interprotein hydrogen bonds is proposed on the basis of the docking simulations between P450cam and Pdx (9). If each hydrogen bond is mediated by 1 water molecule, only 5 water molecules could be explained among 25 or 13 water molecules obtained by osmotic stress. As seen in the case of HEL/Fv D1.3, however, the water-mediated hydrogen bonds form the extensive three-dimensional network that bridges two proteins. Whereas two amino acids separated by 6 Å cannot form the hydrogen bond in general, the water molecule at the intermediate position allows the hydrogen bonding interaction between these two residues; amino acid residue-(3.0 Å)-H_2O-(3.0 Å)-amino acid residue. It might therefore be possible that 25 (in P450cam·Pdx^{red}) or 13 (in P450cam·Pdx^{ox}) water molecules are involved in the hydrogen-bonding network to assist the protein-protein association.

Unfortunately, the crystal structure of P450cam·Pdx complex has not yet been available, and we cannot assign the detailed location of the trapped water molecules at the interface. Among many P450 proteins, the complex structure between P450 and its partner protein has been revealed only in P450BM-3 at 2.03 Å resolution (45). Between the heme and the

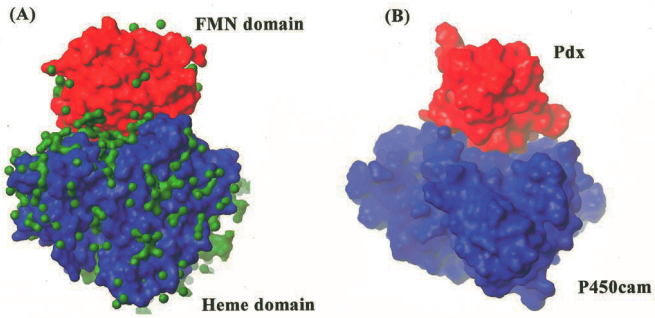

FIG. 7. **Comparison of the crystal structure of P450BM-3 with the computer-simulated structure of the P450cam·Pdx complex.** *A,* the crystal structure of the heme domain (*blue*) complexed with the FMN domain (*red*) in P450BM-3 (45). The water molecules detected in the crystal structure are shown in *green*. *B*, computer-simulated structure of the P450cam·Pdx complex, developed by Pochapsky *et al.* (9). The atomic coordinates of this complex are a gift from Prof. Pochapsky. The regions colored by *red* and *blue* are Pdx and P450cam, respectively. The packing at the complex interface is not perfect, and the cavity at the interface is considered to be filled with water molecules.

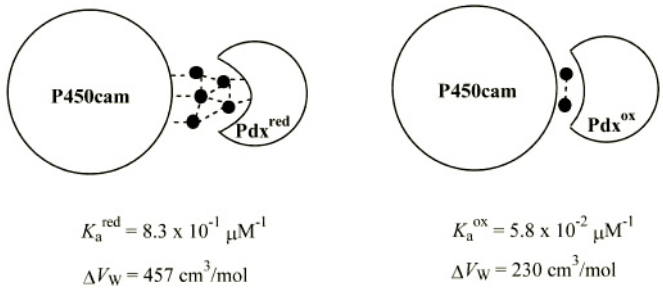

FIG. 8. **Schematic representation of the difference between P450cam/Pdx^{red} and P450cam/Pdx^{ox} complexes.** Interfacial water molecules are depicted as *black circles*. *Dotted lines* are the plausible hydrogen-bonding interactions. The larger number of interfacial water molecules in the P450cam·Pdx^{red} complex would reflect the larger ΔV_W. The difference in the affinities between complexes with Pdx^{ox} and Pdx^{red} is due to the number of the hydrogen-bonding interactions.

FMN domains of P450BM-3, there are two direct hydrogen bonds and several water-mediated contacts. Sevrioukova *et al.* (45) have also argued that well ordered water molecules at the interface serve as hydrogen-bonded bridges between the two domains. Whereas the redox partner is different between P450cam and the heme domain of P450BM-3, the structure of P450cam is similar to that of the heme domain of P450BM-3. It is, therefore, possible that the osmotically labile water molecules are also trapped at the interface of P450cam·Pdx complex to mediate the hydrogen-bonding interaction.

The buried water molecules at the interface are not necessarily involved only in the hydrogen-bonding interactions. In the association of bobwhite quail lysozyme with its antibody HyHEL-5 (37) and of porphyrin-substituted cytochrome *c* with cytochrome *c* oxidase (34), several water molecules occupy the void at the complex interface, which is caused by imperfect packing, resulting in the increase of the shape complementarity. Also in the crystal structure of P450BM-3 (Fig. 7*A*), there are significant numbers of water molecules at the craggy domain-interface. Because of the unavailability of the P450cam·Pdx complex crystal structure, we cannot currently give a definitive conclusion on the number of water molecules involved in the hydrogen bond or in the increase of the shape complementarity. However, the large number of osmotically labile waters suggests that both of these effects may be responsible for the P450cam-Pdx association. Indeed, as seen in the computer-simulated structure of the P450cam·Pdx complex (Ref. 9, Fig. 7*B*), the complex interface is a craggy structure both on P450cam and Pdx, and the packing is not perfect. It can, therefore, be suggested that water molecules fill the cavity at the P450cam·Pdx interface, increasing the shape complementarity and mediating the hydrogen-bonding interactions.

It has been generally believed that for the formation of macromolecular complexes, tighter binding is usually accompanied by a greater extent of dehydration (13–15). In contrast, we find that high affinity binding of ferric P450cam to Pdx^{red} ($K_a^{red} = 8.3 \times 10^{-1}$ μM^{-1}) is accompanied by more water uptake (25 molecules) than the low affinity binding to Pdx^{ox} ($K_a^{ox} = 5.8 \times 10^{-2}$ μM^{-1}, uptake of 13 water molecules). As discussed above, these water molecules are considered to be involved in the formation of the hydrogen-bonding network by filling the cavity at the interface. Therefore, one of the possible explanations for the different ΔV_W between P450cam·Pdx^{red} and P450cam·Pdx^{ox} is that the hydrogen-bonding network at the interface would be more extensive in the P450cam·Pdx^{red} association than the complex with Pdx^{ox}. In terms of the binding energetics, the weaker association of K_a^{ox} than K_a^{red} corresponds to a free energy difference of 6.5 kJ mol^{-1}. Whereas the energetics of the water-mediated hydrogen bonds is experimentally difficult to examine, Williams *et al.* (46) have estimated that a buried water-protein hydrogen bond stabilizes the folded protein by 2.5 kJ mol^{-1}. Langhorst *et al.* (47) have also studied the water-mediated protein-protein interactions in RNase T1 and reported that the free-energy contribution of the interactions of Asn^9 and Thr^{93} through water molecules to the conformational stability does not exceed the absolute value of 1.3 kJ mol^{-1}. In comparison with the direct hydrogen bond (up to about 12.6 kJ mol^{-1} stabilization, Ref. 48), the water-mediated one will be weaker, but the interfacial water molecules can both mediate noncomplementary donor-donor or acceptor-acceptor pairs and connect nonoptimally oriented donor-acceptor pairs. It is, therefore, possible that the redox-dependent affinity difference of as much as 6.5 kJ mol^{-1} is manifested by the rearrangement of about 10 interfacial water molecules as observed.

Actually, the structure of the P450cam·Pdx^{ox} and P450cam·Pdx^{red} complexes are believed to be different. Although the structure of Pdx has been only determined in the oxidized state, it has been reported that there are some structural changes upon the reduction of Pdx^{ox} (4, 49–52). The ^{15}N NMR relaxation measurements have suggested that Pdx^{ox} exhibits higher mobility than Pdx^{red}, especially at residue Asp^{34} forming the ionic pairs with Arg^{109} of P450cam (49). As proposed by Pochapsky *et al.* (51), it is also possible that upon the reduction of Pdx^{ox} the indole ring of Trp^{106} would be partially inserted into a cleft on the surface of the protein. Therefore, these redox-dependent structural and/or dynamics changes in Pdx would lead to a different structure at the complex interface between ferric P450cam and Pdx^{ox} or Pdx^{red} as represented in Fig. 8, resulting in the more extensive hydrogen-bonding network in the ferric P450cam·Pdx^{red} complex.

The molecular recognition by the water-mediated interactions discussed above can also be seen in the restriction enzyme/DNA complex. Robinson and Sligar (53) have suggested the participation of bound waters in the sequence discrimination of substrate DNA by *Eco*RI by using the osmotic pressure method. Whereas *Eco*RI binding occurs more tightly at the recognition site (GAATTC) than the alternate DNA sequence (TAATTC), there are ~70 water molecules in the *Eco*RI-GAATTC complex that are not present in the complex with TAATTC. They have proposed that in the *Eco*RI system the extent of bound water is critical to binding affinity, sequence-specific recognition, and site discrimination during DNA cleavage. As seen in *Eco*RI-DNA recognition, therefore, ferric P450cam can also associate more tightly with Pdx^{red} through

the extensive hydrogen-bonding network mediated by water molecules, which would be broken in the P450cam·Pdx^{ox} complex, resulting in the higher affinity of P450cam with Pdx^{red} compared with Pdx^{ox}.

In summary, this study shows that water molecules can be one of the key players in molecular recognition and probably in redox-dependent affinity between P450cam and Pdx. It is plausible that the extensive hydrogen-bonding network mediated by the intervening water molecules contributes to the redox-dependent affinity of P450cam against Pdx. To gain more insight into the role of water molecules in P450cam-Pdx association, we are currently investigating the dependence of the association on hydrostatic pressure, which can also perturb the hydration state of protein molecules.

Acknowledgment—We are grateful to Prof. Yuzuru Ishimura (Keio University), Prof. Tadao Horiuchi for a gift of the expression vector of the *P450cam* and the *Pdx* genes, and Prof. Thomas C. Pochapsky (Brandeis University) for a gift of the atomic coordinates of the computer-simulated P450cam·Pdx structure. We are also grateful to Dr. Koichiro Ishimori and Dr. Satoshi Takahashi for fruitful discussions and Mr. Takehiko Tosha for experimental advice.

REFERENCES

1. Mueller, E. J., Loida, P. J., and Sligar, S. G. (1995) *Cytochrome P450, Structure, Mechanism, and Biochemistry* (Oritz de Montellano, P. R., ed), pp. 83–124, Plenum Press, New York
2. Davies, M. D., and Sligar, S. G. (1992) *Biochemistry* **31,** 11383–11389
3. Lipscomb, J. D., Sligar, S. G., Namtvedt, M. J., and Gunsalus, I. C. (1976) *J. Biol. Chem.* **251,** 1116–1124
4. Stayton, P. S., and Sligar, S. G. (1991) *Biochemistry* **30,** 1845–1851
5. Stayton, P. S., and Sligar, S. G. (1990) *Biochemistry* **29,** 7381–7386
6. Unno, M., Shimada, H., Toba, Y., Makino, R., and Ishimura, Y. (1996) *J. Biol. Chem.* **271,** 17869–17874
7. Holden, M., Mayhew, M., Bunk, D., Roitberg, A., and Vilker, V. (1997) *J. Biol. Chem.* **272,** 21720–21725
8. Aoki, M., Ishimori, K., and Morishima, I. (1998) *Biochim. Biophys. Acta* **1386,** 157–167
9. Pochapsky, T. C., Lyons, T. A., Kazanis, S., Arakaki, T., and Ratnaswamy, G. (1996) *Biochimie* (*Paris*) **78,** 723–733
10. Roitberg, A. E., Holden, M. J., Mayhew, M. P., Kurnikov, I. V., Beratan, D. N., and Vilker, V. L. (1998) *J. Am. Chem. Soc.* **120,** 8927–8932
11. Sligar, S. G., Debrunner, P. G., Lipscomb, J. D., Namtvedt, M. J., and Gunsalus, I. C. (1974) *Proc. Natl. Acad. Sci. U. S. A.* **71,** 3906–3910
12. Jelesarov, I., and Bosshard, H. R. (1994) *Biochemistry* **33,** 13321–13328
13. Bogan, A. A., and Thorn, K. S. (1998) *J. Mol. Biol.* **280,** 1–9
14. Conte, L. L., Chothia, C., and Janin, J. (1999) *J. Mol. Biol.* **285,** 2177–2198
15. Chothia, C., and Janin, J. (1975) *Nature* **256,** 705–708
16. Aoki, M., Ishimori, K., Fukuda, H., Takahashi, K., and Morishima, I. (1998) *Biochim. Biophys. Acta* **1384,** 180–188
17. Parsegian, V. A., Rand, R. P., and Rau, D. C. (2000) *Proc. Natl. Acad. Sci. U. S. A.* **97,** 3987–3992
18. Di Primo, C. C., Sligar, S. G., Hui Bon Hoa, G., and Douzou, P. (1992) *FEBS Lett.* **312,** 252–254
19. Gunsalus, I. C., and Wagner, G. C. (1978) *Methods Enzymol.* **52,** 166–188
20. Davies, M. D., Qin, L., Beck, J. L., Suslick, K. S., Koga, H., Horiuchi, T., and Sligar, S. G. (1990) *J. Am. Chem. Soc.* **112,** 7396–7398
21. Hintz, M. J., and Peterson, J. A. (1981) *J. Biol. Chem.* **256,** 6721–6728
22. Hintz, M. J., Mock, D. M., Peterson, L. L., Tuttle, K., and Peterson, J. A. (1982) *J. Biol. Chem.* **257,** 14324–14332
23. Kido, T., and Kimura, T. (1979) *J. Biol. Chem.* **254,** 11806–11815
24. Weast, R. C. (1977) *CRC Handbook of Chemistry and Physics* 58th Ed., pp. D228–D231, CRC Press, Inc., Cleveland
25. Rand, R. P., Fuller, N. L., Butko, P., Francis, G., and Nicholls, P. (1993) *Biochemistry* **32,** 5925–5929
26. Furukawa, Y., Ishimori, K., and Morishima, I. (2000) *Biochemistry* **39,** 10996–11004
27. Unno, M., Christian, J. F., Benson, D. E., Gerber, N. C., Sligar, S. G., and Champion, P. M. (1997) *J. Am. Chem. Soc.* **119,** 6614–6620
28. Aoki, M., Ishimori, K., Morishima, I., and Wada, Y. (1998) *Inorg. Chim. Acta* **272,** 80–88
29. Koga, H., Sagara, Y., Yaoi, T., Tsujimura, M., Nakamura, K., Sekimizu, K., Makino, R., Shimada, H., Ishimura, Y., Yura, K., Go, M., Ikeguchi, M., and Horiuchi, T. (1993) *FEBS Lett.* **331,** 109–113
30. Di Primo, C., Deprez, E., Hui Bon Hoa, G., and Douzou, P. (1995) *Biophys. J.* **68,** 2056–2061
31. Harris, D., and Loew, G. (1993) *J. Am. Chem. Soc.* **115,** 8775–8779
32. Marcus, R. A., and Sutin, N. (1985) *Biochim. Biophys. Acta* **811,** 265–322
33. Kornblatt, M. J., Kornblatt, J. A., and Hui Bon Hoa, G. (1993) *Arch. Biochem. Biophys.* **306,** 495–500
34. Kornblatt, J. A., Kornblatt, M. J., Hui Bon Hoa, G., and Mauk, A. G. (1993) *Biophys. J.* **65,** 1059–1065
35. Mauk, M. R., Reid, L. S., and Mauk, A. G. (1982) *Biochemistry* **21,** 1843–1846
36. Kresheck, G. C., Vitello, L. B., and Erman, J. E. (1995) *Biochemistry* **34,** 8398–8405
37. Xavier, K. A., Shick, K. A., Smith-Grill, S. J., and Wilson, R. C. (1997) *Biophys. J.* **73,** 2116–2125
38. Kondo, H., Shiroishi, M., Matsushima, M., Tsumoto, K., and Kumagai, I. (1999) *J. Biol. Chem.* **274,** 27623–27631
39. Spolar, R. S., and Record, M. T., Jr. (1994) *Science* **263,** 777–784
40. Janin, J., and Chothia, C. (1978) *Biochemistry* **17,** 2943–2948
41. Finkelstein, A. V., and Janin, J. (1989) *Protein Eng.* **3,** 1–3
42. Dunitz, J. D. (1994) *Science* **264,** 670
43. Robinson, C. R., and Sligar, S. G. (1996) *Protein Sci.* **5,** 2119–2124
44. Bhat, T. N., Bentley, G. A., Boulot, G., Greene, M. I., Tello, D., Dall'Acqua, W. D., Souchon, H., Schwarz, F. P., Mariuzza, R. A., and Poljak, R. J. (1994) *Proc. Natl. Acad. Sci. U. S. A.* **91,** 1089–1093
45. Sevrioukova, I. F., Li, H., Zhang, H., Peterson, J. A., and Poulos, T. L. (1999) *Proc. Natl. Acad. Sci. U. S. A.* **96,** 1863–1868
46. Williams, M. A., Goodfellow, J. M., and Thornton, J. M. (1994) *Protein Sci.* **3,** 1224–1235
47. Langhorst, U., Backmann, J., Loris, R., and Steyaert, J. (2000) *Biochemistry* **39,** 6586–6593
48. Fersht, A. R., Shi, J. P., Knill-Jones, J., Lowe, D. M., Wilkinson, A. J., Blow, D. M., Brick, P., Carter, P., Waye, M. M., and Winter, G. (1985) *Nature* **314,** 235–238
49. Sari, N., Holden, M. J., Mayhew, M. P., Vilker, V. L., and Coxon, B. (1999) *Biochemistry* **38,** 9862–9871
50. Pochapsky, T. C., Jain, N. U., Kuti, M., Lyons, T. A., and Heymont, J. (1999) *Biochemistry* **38,** 4681–4690
51. Pochapsky, T. C., Ratnaswamy, G., and Patera, A. (1994) *Biochemistry* **33,** 6433–6441
52. Roitberg, A. E. (1997) *Biophys. J.* **73,** 2138–2148
53. Robinson, C. R., and Sligar, S. G. (1998) *Proc. Natl. Acad. Sci. U. S. A.* **95,** 2186–2191